

Original Article

Pathogenicity of p.Phe147del in RET in familial Hirschsprung's disease

Wei Wu*, Kezhe Tan*, Weijue Xu, Jiangbin Liu, Zhibao Lv

Department of General Surgery, Shanghai Children's Hospital, Shanghai Jiao Tong University, Shanghai, China.

*Equal contributors.

Received November 9, 2022; Accepted February 15, 2023; Epub April 15, 2023; Published April 30, 2023

Abstract: Objective: The study aimed to explore the pathogenicity of *RET* p.Phe147del in a Hirschsprung's disease (HSCR) family and facilitate the deeper understanding of HSCR families. Methods: Whole-exome sequencing (WES) was performed to decipher a HSCR family. We used a "GlycoEP" tool to analyze *RET* protein glycosylation. A series of molecular biological approaches including mutated plasmid construction, cell transfection, polymerase chain reaction, immunofluorescence and immunoblotting were introduced to determine the mutation status and altered expression of *RET* as well as its related genes or proteins. MG132 was applied to analyze the mechanism of mutated *RET*. Results: WES and Sanger results revealed that p.Phe147del in-frame mutation (IM) was a potential pathogenic factor for familial HSCR. Moreover, the IM led to disrupted N-glycosylation of *RET* accompanied with protein structural change, resulting in the decreased transcriptional and protein level of *RET*, *CCND1*, *VEGF* and *BCL2*, and the decreased protein level of phosphorylated *ERK* and *STAT3*. Further studies revealed that the IM-evoked *RET* decline was reversed by inhibiting proteasome in a dose dependent manner, thus suggesting that the decrease in intracellular *RET* protein levels interrupted the transportation of *RET* protein from the cytoplasm to the cell surface. Conclusion: The newly found p.Phe147del IM of *RET* is pathogenic to familial HSCR and it disrupts *RET* structure and abundance via the proteasome pathway, representing evidence for the early prevention, clinical diagnosis and treatment of HSCR.

Keywords: Familial Hirschsprung's disease, *RET*, in-frame mutation, protein degradation

Introduction

Hirschsprung's disease (HSCR) is a congenital disease resulting in developmental disorders of the enteric nervous system (ENS) characterized by pathological changes of enteric neural crest cells in the process of proliferation, differentiation and migration. Its incidence rate ranks second in digestive tract malformations in children and the highest cause of mortality is enterocolitis. HSCR is mainly characterized by the loss or dysplasia of neurons and ganglion cells in the intestine [1]. The clinical manifestations of the disease are mainly due to the weakening of the intestinal peristalsis and low and incomplete mechanical obstruction of colon wall, which results in stubborn constipation and abdominal distension. Depending on the presence of concomitant malformations in congenital megacolon, HSCR can be divided into two types: simple and syndrome [2]. The syndrome type is com-

monly associated with trisomy 21 or other organ system malformations, such as gastroenteric malformation, urogenital sinus malformation or congenital cleft lip and palate, congenital heart disease and other malformations. Additionally, it can also be divided into familial or sporadic megacolon based on family disease history [3]. It was the first report in 1948 that Swenson performed the abdominal and perineal pull-out operation to treat congenital megacolon, highlighting that HSCR treatment has entered the era of radical surgery [4]. Therefore, in spite of simple or syndrome type, HSCR treatment is standardized to surgically removing the intestinal segment lacking ganglia and reconstructing the intestinal tract.

Environmental factors such as mycophenolate ester, a semi-synthetic biological inhibitor of guanine nucleotide, which inhibits the development of nerve cells in zebrafish intestine and

Pathogenicity of RET p.Phe147del in HSCR

Table 1. Information of 7 members of a Hirschsprung's disease family

NO	Visiting age	Type	Operation age	Operation type	Prognosis	Sanger results of RET p.Phe147del
1 (III-1)	6 month	Common	1 month	Soave	Good	Mutation
2 (III-2)	12 year	Common	3 month	Soave	Good	Mutation
3 (III-3)	17 year	Long segment	1 month (Phase I) 6 month (Phase II)	Soave	Good	Mutation
4 (II-1)	41 year	Common	1 month	Soave	Good	Mutation
5 (II-2)	45 year	/	/	/	/	No mutation
6 (II-3)	40 year	/	/	/	/	No mutation
7 (II-4)	42 year	/	/	/	/	No mutation

Prognosis follow-up included defecation, enterocolitis, feces, etc. HSCR: Hirschsprung's disease.

also selectively inhibits the proliferation and migration of intestinal nerve precursor cells in mice, have been reported to induce symptoms similar to HSCR [5]. In addition, many pieces of literature show that vitamin B12 deficiency and anti-folate drugs such as methotrexate can increase the incidence rate of HSCR [6].

However, HSCR mainly follows a dominant inheritance pattern, and the non-Mendelian genetic model displays reduced penetrance or recessive inheritance to more complex sporadic cases [3]. To date, it has been found that activation or inactivation mutations of many genes, such as ECE, RET, END3, EDNRB, SRY-BOX transcription factor 10 (SOX10), glial cell line-derived neurotrophic factor (GDNF), neurotrophic factor, transcription factors that functions similarly to paired homologous gene 2B (PHOX2B) and KIAA12794, can lead to HSCR [7]. In 2012, Mantovani et al. used CRISPR/Cas9 technique to edit the RET mutation in a vitro model, significantly recovering the impaired intestinal neural crest cells. It indicates that RET gene mutation plays a crucial role in the pathogenesis of HSCR [8]. Previous reports have shown that at least 20% of HSCR cases are caused by mutations in the proto-oncogene RET, highlighting its potential as the main gene involved in the aetiology of HSCR. The effective mutation of the RET gene is often caused by coding region variation and non-coding region enhancer variation. Transcription factors including SOX10 and PHOX2B promote or enhance RET expression in enteric neural crest cells, and a knockout of any one of these factors will lead to intestinal gangliosis [7, 9]. The signal pathways regulated by RET are involved in the pathogenesis of HSCR at multiple levels and dimensions, including

embryology, genetics, transcriptional regulation, protein function and epigenetics.

To further address the genetic issue, we focused on a HSCR family in our center. The newly found p.Phe147del IM of RET was proved to play a role in pathogenesis of familial HSCR, providing valuable evidence to understand the early prevention, clinical diagnosis and treatment of HSCR.

Materials and methods

Study design

The ethical review of Children's Hospital Affiliated to Shanghai Jiaotong University approved this study (2020RY022-E01 and 2022RY022-E01). The parents or legal guardians of the child signed the informed consent form. Main clinical data of the HSCR family were summarized ([Supplementary Figure 1](#) and [Table 1](#)). Haematoxylin and eosin (H&E) staining and immunohistochemistry were performed on the sections of the dilated and stenotic bowels of the proband. In addition, we randomly collected 20 samples of non-familial HSCR from our center ([Supplementary Table 1](#)).

Sample collection and whole exon sequencing (WES)

The procedures were previously reported [10]. Briefly, peripheral blood was collected and genomic DNA was extracted following the manufacturer's instructions (Genomic DNA Extraction Kit, QIAGEN, Germany). The samples that passed quality control (QC) in polymerase chain reaction (PCR) assay were applied to the constructed library. Illumina HiSeq 2500, X Ten or NovaSeq platform PE150 was used for

Pathogenicity of RET p.Phe147del in HSCR

sequencing analysis. The ANNOVAR software was used to annotate the variation results.

Sanger sequencing

The primers were devised using the Primer 5.0 and Oligo 1.3 software (forward primer sequence: 5'-GCTTGAGGAACATGAGCTGAC-3'; reverse primer sequence: 5'-GCAGAGTAATC-ACCAGCTCC-3'). The forward and reverse primers, 10x buffer dNTPs, template DNA, LATAPDNA enzyme and double distilled water were added in order and then underwent PCR assay.

RET glycosylation analysis

The influence of p.Phe147del on the glycosylation of RET was evaluated using GlycoEP, which predicts N-glycosylation and O-glycosylation [10]. Using the protein glycosylation database NetOGlyc: Prediction of O-GalNAc (mucin type) (<http://www.cbs.dtu.dk/services/NetOGlyc/>), the glycosylation sites in the main protein were identified. Furthermore, on searching for N-glycosylation and O-glycosylation site conservative sequences in the protein sequence, the characteristic sequence of the amino acid of the N-glycosylation site conservative sequence was identified using the Asn-x-ser/thr method.

Cell culture, plasmid construction and transfection

Human embryonic kidney cells 293T were cultured in Dulbecco's modified eagle medium (DMEM) supplemented with 10% fetal bovine serum. When 80% confluence was reached, they were sub-cultured in a ratio of 1:3. The constructs were built as previously described [11]. According to the target gene and its mutants, the target gene CDS fragments were obtained using whole genome synthesis. After PCR amplification, the target gene was molecularly cloned to the receptor strain. The reconstructed plasmid was used to transiently transfect cells for 48 hours with the help of Lipofectamine 2000 and the RET overexpression was verified using Q-RT-PCR and Western blot.

Q-RT-PCR

PCR primers were designed and synthesized according to the target gene. The primers were as follows: RET: forward primer (5'-GCG-

AGAATTCGGCGGAATTCGGCAGTAAATGGCAG-TACCC-3') and reverse primer (5'-GCGAGGATTCGACGGGATCCACAGACTGTCCCCACACAGC-3'); GFRa-1: forward primer (5'-ACTCCTGGA-TTTGCTGATGTCGG-3') and reverse primer (5'-CGCTGCGGCACTCATCCTT-3'); Cyclin D1: forward primer (5'-GCTGCGAAGTGGAAACCATC-3') and reverse primer (5'-CAGGACCTCCTTCTGCACAC-3'); VEGF: forward primer (5'-CGAAACCATGAACCTTCTGCTGTC-3') and reverse primer (5'-TCACCGCCTCGGCTTGTCACAT-3'); BCL-2: forward primer (5'-TACCGTCGTGACTTCGCAGAG-3') and reverse primer (5'-GGCAGGCTGAGCAGGGTCTT-3'). After obtaining the cDNA, it was diluted 5-fold. Then, 1 µL of it was used as the template during PCR, which was performed according to the following conditions. The PCR system contains template, 1 µL; 10 × PCR buffer, 2.5 µL; dNTP, 2.5 µL; forward/reverse primer, 1.2 µL; easy Taq enzyme, 0.2 µL; water supplement; total volume, 25 µL. The PCR condition was as following: 94°C for 4 min, 94°C for 30 s, 55°C for 30 s, 72°C for 30 s, 72°C for 4 min and 16°C for holding [12].

Western blot

Proteins were extracted and quantified in RIPA buffer as previously described [13]. The lysates were separated by sodium dodecyl sulfate polyacrylamide gel electrophoresis (SDS-PAGE) and transferred to polyvinylidene difluoride (PVDF) membrane. The membranes were blocked in 5% skimmed milk buffer and incubated with antibodies of target proteins (RET 1:500, abcam, #ab134100; GARF1 1:1000 #11711-1-AP; Cyclin D1 1:1000, abcam, #ab-134175; VEGF 1:1000, abcam, #ab32152; Bcl-2 1:500, abcam, #ab32124; ERK 1:1000, abcam, #ab32537; STAT3 1:1000, abcam, #ab68153) and internal reference proteins overnight at 4°C. The membranes were then rinsed thrice with 1 × TBST and incubated with the secondary antibody at room temperature for 1-2 h. The blots were developed by Luminescent Image Analyzer (Fujifilm, LAS-4000) after incubation with enhanced chemiluminescence reagents (Millipore, WBKLS0500). Image J software was used to collate data and conduct subsequent analysis.

Immunofluorescence

Human 293T cells were divided into four groups and transfected with RET p.Phe147del plasmid. A 12-well culture plate was used for

Pathogenicity of RET p.Phe147del in HSCR

triplicate. Different concentrations of MG132 (Sigma M7449) were added to each group of cells for 12 hours and immunofluorescence staining was performed when the cell confluence was approximately 80%. Cells were washed with preheated (37°C) 1 × PBS for 3 times. 4% paraformaldehyde was added to fix the cells for 20 min and the cells were blocked with 0.01% Triton and 5% BSA buffer for 30 min at room temperature. Primary antibodies against RET (1:500, abcam, #ab134100) were incubated in dark overnight at 4°C and secondary antibodies (Abcam, #ab6046) were incubated at room temperature for 2 h. The samples were routinely rinsed 3 times with 1 × PBS for 10 min each time at room temperature before the blocking and antibody incubation steps. Subsequently, DAPI was added followed by an anti-quenching agent at room temperature. The staining of the cell nucleus and target protein under different fluorescence conditions was observed using an inverted phase contrast microscope and fluorescence microscope. ImageJ software was used to analyse the images obtained and merge the nuclear staining photos with the corresponding target protein staining photos for further analysis.

Cell signal pathway

We additionally measured the transcriptional and protein level of cyclin D1 (CCND1), VEGF and BCL2 that might be part of the downstream signal pathway of RET [14, 15]. The protein expression of p-ERK/ERK and p-STAT3/STAT3 that were also reported to be the downstream signal pathway [16] was analyzed as well.

Statistics

GraphPad Prism 9 (GraphPad Software) software was used to visualize the experimental data. The quantitative data are shown as means ± standard error. Unpaired two-tailed t test was used in comparisons between two groups and one-way ANOVA was used in comparisons among more than two groups for all experiments. $P < 0.05$ was considered as statistically significant.

Results

Diagnosis of congenital HSCR in a family

The number of ganglion cells in the submucosa of the intestinal wall and the myenteric plexus

of the expanded segment was normal and showed good development. The ganglion cells in the submucosa of the intestinal wall and the myenteric plexus of the expanded segment gradually decreased from the expanded segment to the narrow segment, accompanied by an increase in dense wavy unsheathed nerve fibres and Schwann cells and a complete absence of ganglion cells in the narrow segment (**Figure 1A, 1B**). Combined with immunohistochemical results (CD56, NSE, S100, SYN, β -Catenin), the diagnosis of HSCR was verified (**Figure 1C-E**). Immunohistochemistry of the stenosis segment, CD56, NSE, S100, β -catenin, Bcl-2 and SYN (**Figure 1E**) revealed that ganglion cells were negative and some nerve fibres were positive. Furthermore, no ganglion cells were found in the nerve plexus and the number of thickened nerve trunks was more than that of the expanded segments.

Detection of pathogenic genes in the members of one HSCR family using WES and evaluation of 20 sporadic HSCR patients

To identify rare pathogenic variants of familial HSCR in gene coding or splicing regions, we sequenced all exons of the seven family members (II-1, II-2, II-3, II-4, III-1, III-2 and III-3). We detected 239,225 mutations, of which at least one family member's allele differed from the reference genome, including 217,172 substitutions and 22,053 insertions and deletions (**Supplementary Table 2**). For the three affected boys (III-1, III-2 and III-3), Mendel's error estimates are approximately 1.10%, 1.43% and 1.33%, respectively, which indicates that these variables have high reliability. As hereditary HSCR is very rare in the general population, there will likely be few pathogenic variations in the healthy population. To identify rare variants, we first obtained their minor allele frequencies (MAF) from the gnomAD database. By excluding non-coding and synonymous variants, we screened out 1059 rare variants in the family (MAF < 0.1%). Moreover, as HSCR can be inherited through autosomal dominant and recessive patterns, autosomal dominant and recessive variations were considered. Among homozygous and biallelic variants, four patients did not share the recessive variant. Under the assumption of autosomal dominant inheritance, incomplete female II-4 was speculated to be the carrier of the pathogenic variant due to incomplete penetrance. Finally, we identified 18 major variants (**Supplementary Tables 2, 3**),

Pathogenicity of RET p.Phe147del in HSCR

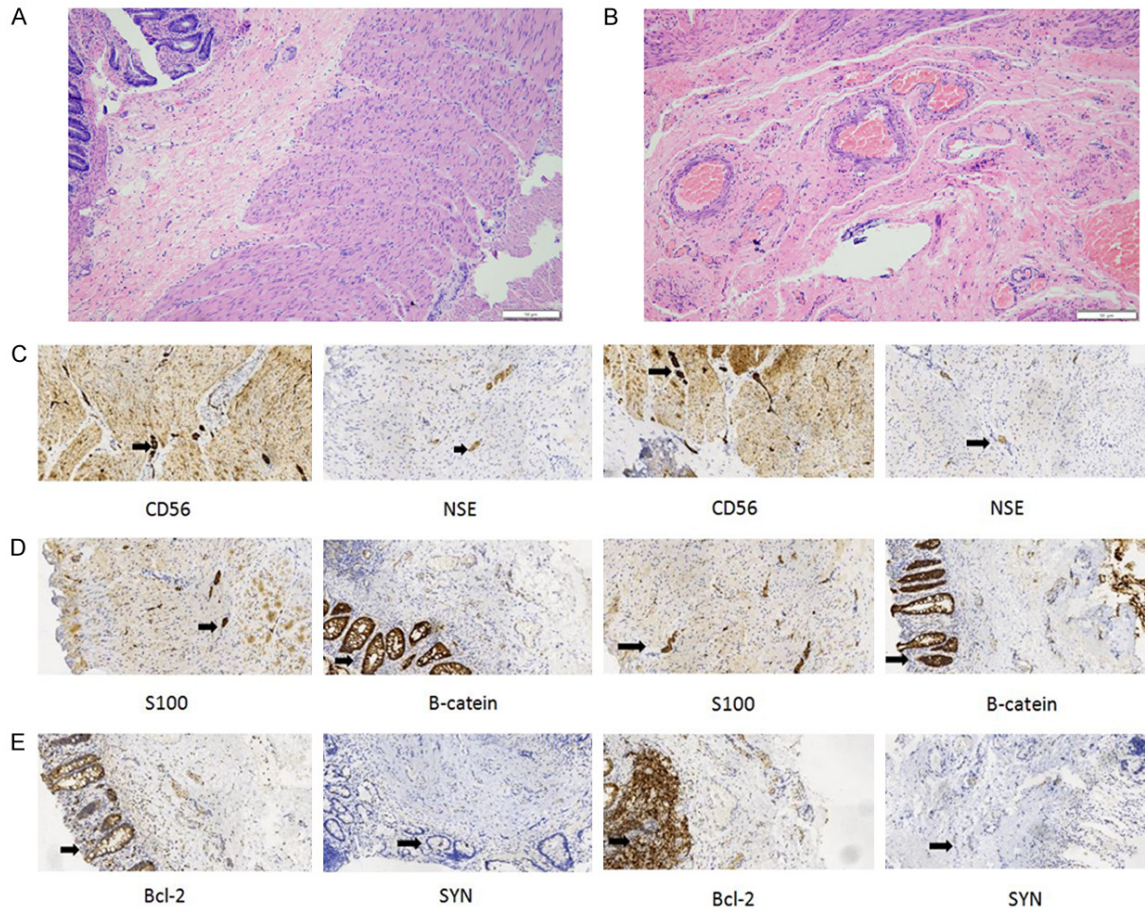


Figure 1. Imaging examination results and immunohistochemical results of the dilated intestinal wall.

including 14 missense mutations, 1 nonsense mutation, 2 frameshift mutations and 1 whole code mutation.

To identify pathogenic variants, we used bioinformatics tools [17] such as SIFT, PolyPhen, MutationTaster, M-CAP, DDIG-in and SIFT indel to evaluate the pathogenicity of the 18 main variants obtained. For the 14 missense variants, we used SIFT (≤ 0.05), PolyPhen (≥ 0.957), MutationTaster (Disease causing) and M-CAP (> 0.025) for filtering, which revealed CAPN9, GLYCTK and DRD5 as potentially pathogenic variants. DDIG-in and SIFT Indel prediction algorithms also identified RET, FANCI and CALN1 Indels to be potentially pathogenic. Additionally, the nonsense mutation of NPHP3 was also identified as potentially pathogenic by MutationTaster and DDIG-in. Thus, seven genes, namely CPN9, GLYCTK, DRD5, NPHP3, FANCI, CALN1 and RET, were identified to have

potential HSCR pathogenicity. To evaluate the relationship between these mutations and HSCR, we conducted a comprehensive literature search on the seven potentially pathogenic genes. First, we found that the p.Phe147del mutation in the *RET* gene is the most common pathogenic gene in HSCR. Nonetheless, other genes, such as GLYCTK [18], DRD5 [19], NPHP3 [20] and FANCI [21], were also pathogenic for some recessive or polygenic rare diseases, such as D-glycosuria, attention deficit hyperactivity disorder, Meckel syndrome and Fanconi anaemia; however, these genes were excluded in further analyses owing to their recessive genetic characteristics.

In addition to the HSCR family, we collected clinical data and performed Sanger sequencing for 20 sporadic HSCR patients, showing that p.Phe147del IM was detected in only 5% of HSCR patients (Supplementary Table 1).

Pathogenicity of RET p.Phe147del in HSCR

p.Phe147del affects RET protein expression

We constructed a GFRA1 plasmid and RET wild type plasmid. Based on the RET wild type sequence, we constructed a RET p.Phe147del plasmid, RET p.L56M and p.W85X plasmid, wherein RET p.L56M is a known mutation that does not affect the expression and function of RET and RET p.W85X is a known inactivation mutation that inhibits RET protein expression (**Figure 2A**). The core fragments of the above plasmids were obtained using whole genome synthesis and identified via sequencing (**Figure 2B** and **2C**). Furthermore, sequencing analyses confirmed the deletion of phenylalanine at position 147 in the RET p.Phe147del plasmid, amino acid change from leucine at position 56 to methionine in L56M and tryptophan at position 85 to asparagine in RET p.L56M and RET p.W85X, respectively (**Figure 2D**).

As shown in **Figure 3A**, compared with wild-type RET, RET p.Phe147del, RET p.L56M and RET p.W85X had lower mRNA expression; however, no significant difference was observed among the expression levels of each mutant. Then, RET p.Phe147del, RET p.L56M and RET p.W85X were co-expressed with GFRA1. The expression of RET at the mRNA level and its regulation on downstream genes were detected using q-RT-PCR. As shown in **Figure 3B**, the co-expression of GFRA1 and RET-WT significantly activated the expression of cyclin D1, VEGF and BCL2, which are downstream of RET. Meanwhile, the activation efficiency of RET p.L56M and RET-WT was the same, whereas RET p.Phe147del and RET p.W85X inhibited the activation of RET downstream genes. Thus, the expression of related genes returned to the background level before GFRA1 co-expression. These findings indicate that the mutation of p.Phe147del has a serious impact on the expression or function of RET protein, inhibiting its downstream signalling functionality. It is speculated that the inactivation mutation at the RET147 site inhibits the binding of GFRA1 and its tyrosine kinase receptor complex with RET protein, thereby inhibiting the activation of RET downstream signalling pathways and consequently leading to the lack of proper ganglion cells in the intestinal segment (narrow segment) of HSCR.

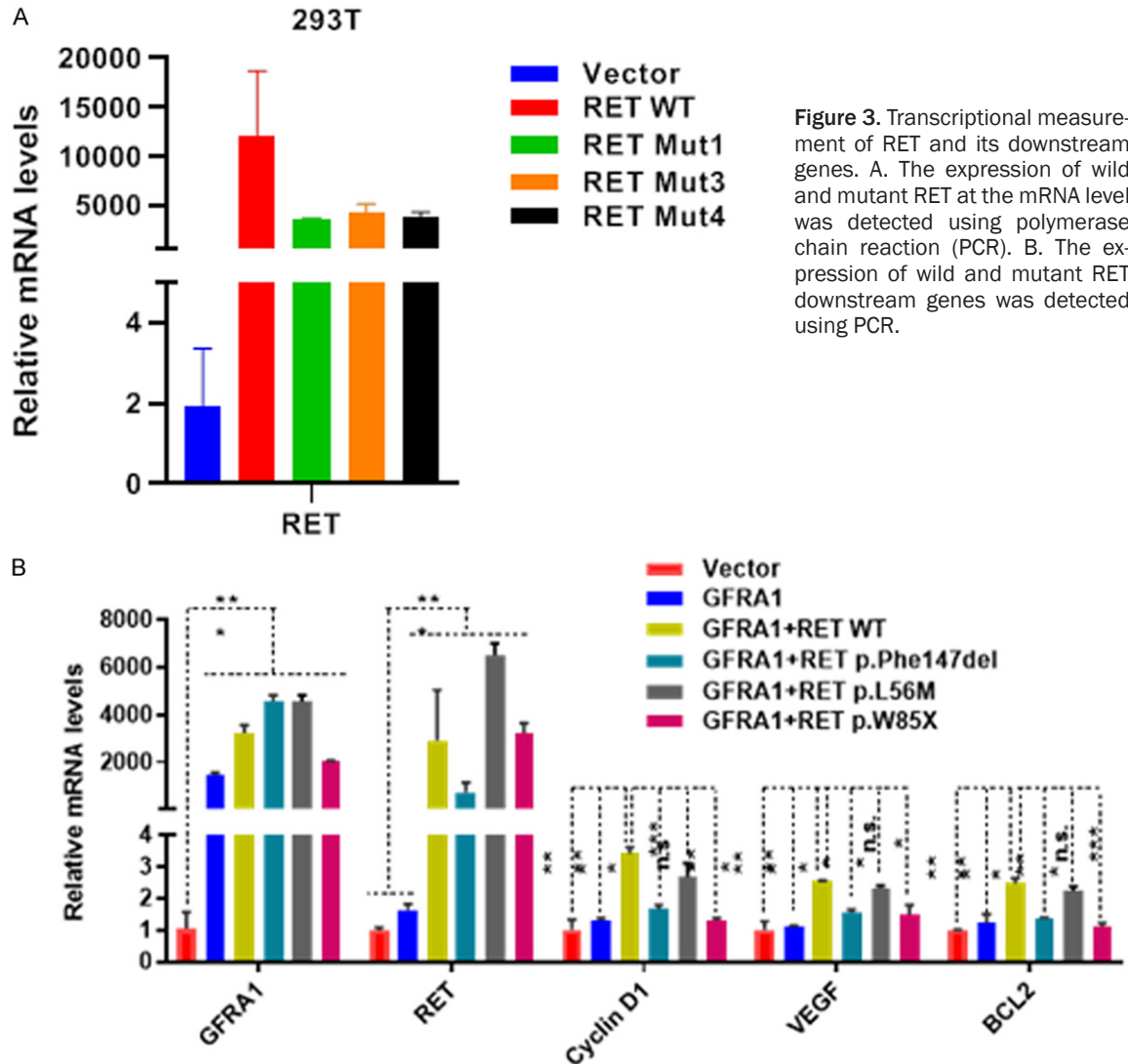
p.Phe147del reduces RET protein expression and downstream regulation

According to the results of binding protein detection, we speculate that the stability of p.Phe147delRET protein was seriously affected by the mutation, which needs further experimental verification. Similarly, we first overexpressed RET p.Phe147del and RET p.L56M and RET p.W85X, respectively. The expression of RET at the protein level was detected using western blot, and the phosphorylated RET was also detected to evaluate its phosphorylation activation. As shown in **Figure 4A** and per previous literature, RET p.L56M is a mutation reported to not affect RET expression and activation, whereas RET p.W85X mutation significantly affects RET protein expression. Furthermore, our newly identified p.Phe147del mutation also makes RET undetectable at the protein level, regardless of its phosphorylation status. Then, RET p.Phe147del, RET p.L56M and RET p.W85X were co-expressed with GFRA1, and the activation of cyclin D1, VEGF and BCL2, which are important downstream factors of RET, at the protein level was detected using western blot. As shown in **Figure 4B**, the co-expression of GFRA1 and RET-WT significantly increased the expression of cyclin D1, VEGF and BCL2 downstream of RET at the protein level, indicating the activation of the RET signalling pathway. The activation efficiency of L56M and RET-WT on downstream signals was consistent. RET p.W85X maintained some activity on some downstream targets, while RET p.Phe147del inhibited the activation of the downstream factors of RET. The above experimental results show that p.Phe147del mutation induces a significant decrease in RET protein expression and the loss of signal transduction function, which is a typical inactivation mutation of the RET signalling pathway.

p.Phe147del induces RET protein degradation via the proteasome pathway

GDNF is an endogenous ligand of GFR α 1, which can activate RET signalling pathway and lead to the phosphorylation activation of downstream ERK and STAT3 signalling pathways. We used this model to evaluate the function of RET p.Phe147del. As shown in **Figure 4C**, the addition of exogenous GDNF stimulated the phos-

Pathogenicity of RET p.Phe147del in HSCR



p.Phe147del increased significantly with the addition of MG132 until it reached a significantly high expression level.

The immunofluorescence method was used to further verify this change in expression levels after MG132 addition. As shown in **Figure 4E**, the expression of RET increased significantly with the increase in MG132 concentration. This result suggests that RET p.Phe147 mutation does express the protein; however, it is degraded through the proteasome pathway owing to its instability. Hence, RET protein cannot be successfully expressed and transported to the cell surface.

Prediction of RET p.Phe147del protein structure

We simulated the protein structure of RET p.Phe147del in silico and characterized the sta-

bility data. mUpro calculates the Gibbs free energy of the wild type first followed by that of the mutant type. This process lasts for 50 cycles. After the program is completed, the $\Delta\Delta G$ data is obtained. If $\Delta\Delta G$ value is negative, that is, the free energy of the mutant is higher than that of the wild type, it indicates that the stability of the mutant is reduced. As shown in **Figure 5A**, for the p.Phe147del mutation, the free energy increased significantly ($\Delta\Delta G = -1.8998757$), indicating that the stability is reduced, which is consistent with our previous results.

The p.Phe147del whole code mutation of RET potentially affects the structure of RET protein

We used ClusterX-2.1-win software to compare RET mutant amino acids with other homologous species: chimpanzees (*Pan troglodytes*),

Pathogenicity of RET p.Phe147del in HSCR

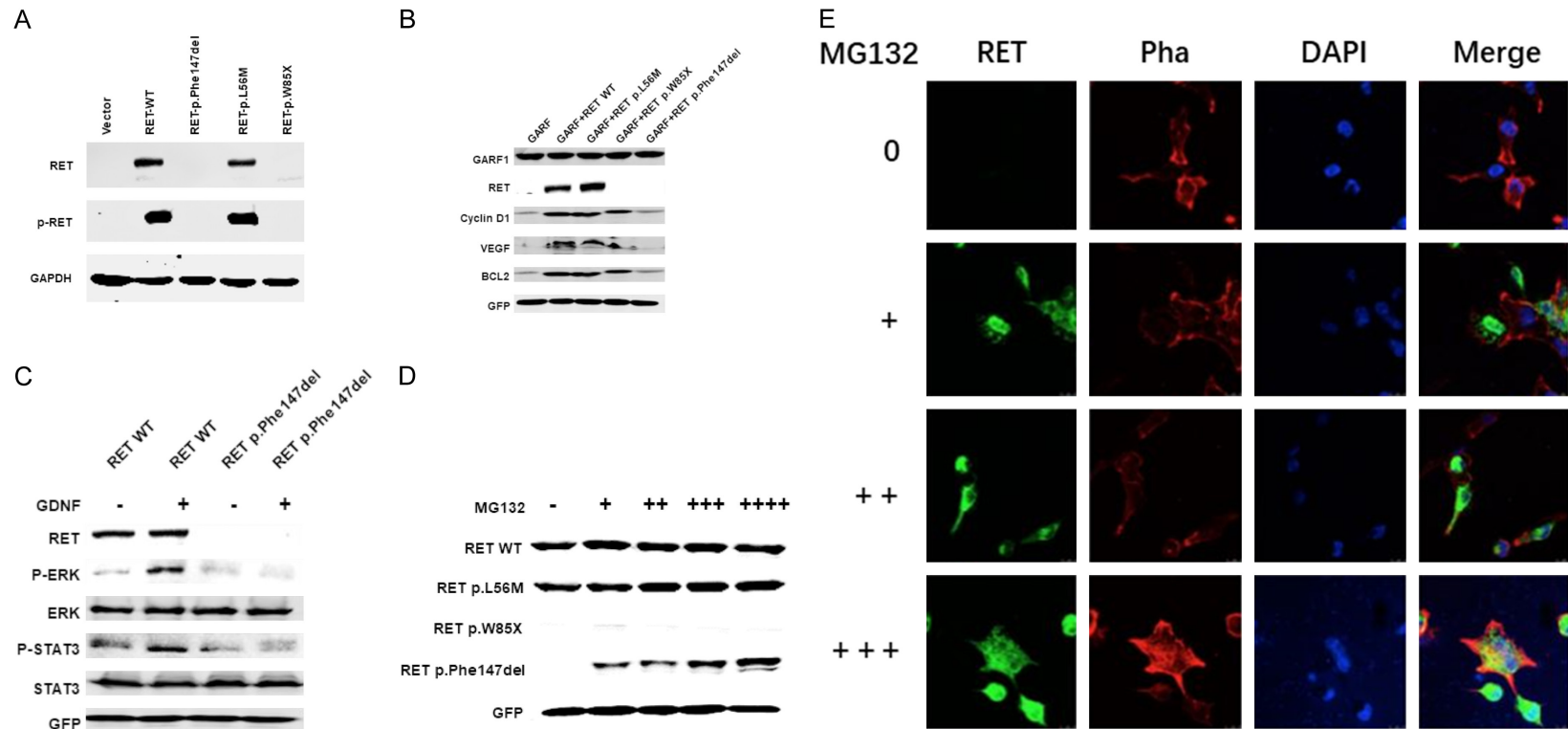


Figure 4. Immunoblots of RET and its downstream proteins and immunofluorescence of RET expression. A. Western blot (WB) was used to detect the expression of wild and mutant RET at the protein level. B. WB was used to detect the expression of wild and mutant RET downstream proteins. C. WB was used to detect the phosphorylation activation of wild and mutant RET downstream proteins stimulated by GDNF. D. WB was used to detect the expression of wild and mutant RET proteins when MG132 inhibited the proteasome activity. E. Immunofluorescence of RET expression induced by MG132 at different concentrations. RET p.Phe147del was overexpressed in 293T cells and was treated with MG132 of different concentrations simultaneously, which were analysed using immunofluorescence.

A

Structure stability prediction for mutation:

Mutation Request:
 Name: RETDEL
 Sequence:

```

MAKATSGAAGRLRLLLLLLPLLGKVALGLYFSRDAYWENLYVDQAAGTPLLIVHALRDAP
EEVPSFRLGQHLGYTYKTRLEHNNWICIQEDTGLLYLNRSLDHSWEKLSVRNRGFPLLT
VYLKVFSLPSTSLRBEBCQWPGCARVYFSPFNTSFFACSSLKPRELCPETRPFRRIENR
PPGTFHQFRLLPVQFLCPNISVAYRLLBEGGLPFRCAPDSEVSTRWALDREQREKYELV
AVCTVHAGAREEVMVPPFVTVYDEDDSSAPTFPAGVDTAASAVVEFKRKEDEVVAITLRFVD
ADVVPASGELVRRYITSTLLPGDTWAQQTFRVEHVFNETSVQANGSFVRATVHDYRLVLNR
NLSISENRIMQLAVLVMDSDFQPGAGVLLLHFNVSVLPVSLHLPSTYSLSVSRARRFA
QIGKVCVENCAFGSINVOYKLSHSGANCSLGGVVTSAEDTSGILFVNDTKALRRPKCAE
LHYMVVATDQTSRQAQALLVTVVYEGSYVAEEAGCPLSCAVSKRRLECEEGGLGSPVGR
CEWRQDCKGIRTRMFTCSPTKTCPDGHCDVVEVDQINICPQDCLRGSIYVGGHEPCEPR
GKAGYTCNCFPEEEKCFCEPEDIQDPLCDEL CRTVIAAAVLFSTIVSVLLSARCIHCY
HKFAHKPPISSAEMTFRRPAQAFPVSYSSGARRFSLDSMEWQVSVDAFKILEDPKWFFP
RKNLVLGKTLGEBEFGKVVKATAPHLKGRAGYTTVAVKMLKENASPSSELDLSEFNVLK
QVNHVHYIKLYGACSDQGPLLLITVEYAKYGLRGLRESRKVGPGYLGSGGSRNSSLDH
PDERALTMGDLISFAWQISQGMQYLAEMKLVHRDLAARNILVAEGRMKKISDFGLSRDYY
EEDSYVKRSQGRIPVKWMAIESLFDHIYTTQSDVWVSPGVLWEIVTLGGNPPYGPPIPERL
FNLLKGTGRMERPDNCSEMYRLMLQCWVQEPDKRPFVADISKDLEKMMVKRRDYLDLAA
STPDSLSLIYDDGLSEETPLVDCNNAFLPRALPSTWIENKLYGRISHAFTRF
    
```

Position: 147
 Original Amino Acid: F
 Substitute Amino Acid:

Prediction Results:

1. Predicted both value and sign of energy change using SVM and sequence information only (Recommended)
 detaI delta G = -1.8998757 (DECREASE stability)
2. Prediction of the sign (direction) of energy change using SVM and neural network with a smaller sequence window

Method 1: Support Vector Machine, use sequence information only.
 Effect: DECREASE the stability of protein structure.
 Confidence Score: -0.67201025

Method 2: Neural Network, use sequence information only.
 Effect: DECREASE the stability of protein structure.
 Confidence Score: -0.812966722741349

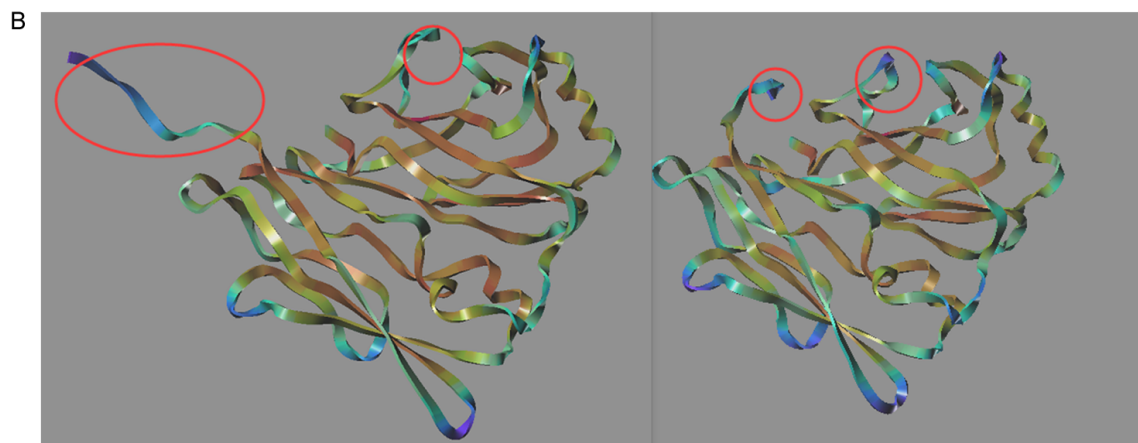


Figure 5. The prediction of protein stability and the structural change of RET. A. The prediction of protein stability of RET p.Phe147del. B. The structural change of wild-type and p.Phe147del RET.

Macaca mulata, dogs (*Canis lupus familiaris*), cattle (*Bos Taurus*), mice (*Mus musculus*), brown mice (*Rattus norvegicus*), chickens (*Gallus gallus*), and *Xenopus tropicalis* (<http://www.ncbi.nlm.nih.gov/homologene>). The am-

ino acid sequences were compared to analyse the conservatism of mutant amino acids in the process of species evolution. MutationTaster (<http://www.mutationtaster.org>) (Protein reference ID: P000471; protein reference trans-

Pathogenicity of RET p.Phe147del in HSCR

cript ID: ENST000000355710) predicts the impact of gene mutation on protein function based on a score. According to the known RET protein structure model, the post-mutation model of 147 site was constructed. Furthermore, Swiss PdbViewer software was used to analyse the changes in protein spatial structure caused by amino acid changes before and after RET gene mutation. The results suggested the presence of a hydrogen bond between nonpolar hydrophobic Asn424 and Pro421 in the wild type RET protein. After the mutation to the polar hydrophilic Asn424, the original hydrogen bond did not change, but another hydrogen bond was added to the same part of Pro421, resulting in a changed protein structure. Furthermore, it is predicted that the abnormal change in threonine-arginine synthesis will lead to an abnormal structure of RET protein after mutation (**Figure 5B**).

Discussion

HSCR is a polygenic defect characterized by complete absence of neuronal ganglion cells in a portion of the intestinal tract [5]. In this study, we performed WES on seven members of a HCSR family and 20 non-familial HSCR patients to identify the p.Phe147del IM of RET gene playing a role in reduced expression of RET and its downstream targets. The IM-induced RET decrease was associated with disrupted RET glycosylation and regulated by the proteasome pathway. These findings conclude the pathogenetic role of p.Phe147del IM of RET and provide further insight into deeper understanding of HSCR.

RET mutations are critical in the pathogenesis of HSCR in both humans and mice as previously reported, such as RET(N394K) in humans [22], single-nucleotide polymorphism (SNP) rs2435357 in humans [23] and Ret(S812F) in mice [24]. Our study first identified the new p.Phe147del IM of RET by WES in 7 members from a HCSR family and evaluated the IM in 20 sporadic HSCR patients in Shanghai Children's Hospital. Notably, less than 1.5% of studies (11 studies in mainland China and 804 studies in total, calculated in *Web of Science*) concerning RET mutations and HSCR were conducted in mainland China. Therefore, our study provides some evidence in HSCR patients in China.

Previous studies showed that RET mutation disturbed glycosylation and affected phosphorylation on GDNF activation, thus playing a role in the pathogenesis of HSCR [3, 10]. Our study revealed the disrupted RET glycosylation by the p.Phe147del IM. In addition, several studies indicated that RET acts as a membrane receptor of tyrosine kinase (RTK) family and is bound to GDNF, activating the downstream pathways that play a role in neural cell growth and survival. We measured the declined markers of cell growth and survival such as CCND1, VEGF and BCL2 [25, 26]. In cancer research, RTK signaling represents the activation of phosphorylated ERK1/2 and STAT3 [25], and STAT3 acts as a transcription factor that binds to the promoter of RET [27, 28], thus potentially forming a positive feedback loop between RET and STAT3. Our results showed the decreased protein level of p-ERK and p-STAT3 in the p.Phe147del IM cells, providing some evidence for this claim.

The ubiquitin-proteasome pathway is the major proteolytic way in eukaryotic cells [29]. MG132 is an effective and reversible cell permeable 20S proteasome inhibitor, which is commonly used to study protein degradation. Our results showed that the p.Phe147del IM degraded RET protein via the ubiquitin-proteasome pathway. Furthermore, *in silico* structural analysis for p.Phe147del RET represented the reduction of intracellular RET protein stability with $\Delta\Delta G = -1.8998757$.

Some limitations and future plan of our study should be noted. Due to the lack of a large number of familial HSCR cases, we only investigated 7 members in one family. We will collaborate with other hospitals to enroll more familial HSCR patients. In addition, we failed to perform experiments to verify the disrupted RET glycosylation in the p.Phe147del IM status, but we aimed to modify the conditions and accomplish the glycosylation assay in the future. Notably, more cell function tests and animal model studies need to be performed in the next project.

In summary, p.Phe147del whole code mutation leads to a significant reduction in RET protein expression and loss of corresponding signal transduction function. It is a typical inactivation mutation of the RET signalling pathway, wherein the stability of the RET protein is affected. It is degraded through the proteasome pathway,

Pathogenicity of RET p.Phe147del in HSCR

which ultimately leads to the reduction of the mutated RET protein and the failure to activate the downstream signalling pathway. These results provide potential important value for enriching the relevant theories of HSCR pathogenesis and providing laboratory evidence for the early prevention and clinical diagnosis and treatment of HSCR.

Conclusion

The newly identified p.Phe147del IM of RET leads to a type of familial HSCR by disrupting RET expression, glycosylation, structure and its downstream pathways via the proteasome pathway, providing evidence for prevention, diagnosis and treatment of HSCR.

Acknowledgements

This work was supported by Shanghai Health Planning Commission Grant (20214Y04976).

The patient (or parent or guardian) provided written informed consent for publication.

Disclosure of conflict of interest

None.

Abbreviations

CCND1, cyclin D1; DMEM, Dulbecco's Modified Eagle Medium; ENS, Enteric Nervous System; GDNF, Glial Cell Line-Derived Neurotrophic Factor; H&E, Haematoxylin and Eosin; HSCR, Hirschsprung's Disease; IM, In-frame Mutation; MAF, Minor Allele Frequencies; PCR, Polymerase Chain Reaction; PHOX2B, Paired Homologous gene 2B; PVDF, Polyvinylidene Difluoride; QPCR, Quantitative PCR; Q-RT-PCR, Quantitative Reversed Transcription PCR; QC, Quality Control; RTK, Receptor Tyrosine Kinase; SDS-PAGE, Sodium Dodecyl Sulfate Polyacrylamide Gel Electrophoresis; SNP, Single-Nucleotide Polymorphism; SOX 10, SRY-BOX Transcription Factor 10; WES, Whole Exon Sequencing.

Address correspondence to: Zhibao Lv, Department of General Surgery, Shanghai Children's Hospital, Shanghai Jiao Tong University, Shanghai, China. E-mail: zhibaoLv@sohu.com

References

[1] Soret R, Schneider S, Bernas G, Christophers B, Souchkova O, Charrier B, Righini-Grunder F,

Aspirot A, Landry M, Kembel SW, Faure C, Heuckeroth RO and Pilon N. Glial cell-derived neurotrophic factor induces enteric neurogenesis and improves colon structure and function in mouse models of hirschsprung disease. *Gastroenterology* 2020; 159: 1824-1838, e1817.

[2] Tilghman JM, Ling AY, Turner TN, Sosa MX, Krumm N, Chatterjee S, Kapoor A, Coe BP, Nguyen KH, Gupta N, Gabriel S, Eichler EE, Berrios C and Chakravarti A. Molecular genetic anatomy and risk profile of Hirschsprung's disease. *N Engl J Med* 2019; 380: 1421-1432.

[3] Sribudiani Y, Chauhan RK, Alves MM, Petrova L, Brosens E, Harrison C, Wabbersen T, de Graaf BM, Rugenbrink T, Burzynski G, Brouwer RWW, van IWFJ, Maas SM, de Klein A, Osinga J, Eggen BJL, Burns AJ, Brooks AS, Shepherd IT and Hofstra RMW. Identification of variants in RET and IHH pathway members in a large family with history of Hirschsprung disease. *Gastroenterology* 2018; 155: 118-129, e116.

[4] Swenson O, Neuhauser EB and Pickett LK. New concepts of the etiology, diagnosis and treatment of congenital megacolon (Hirschsprung's disease). *Pediatrics* 1949; 4: 201-209.

[5] Diposarosa R, Bustam NA, Sahiratmadja E, Susanto PS and Sribudiani Y. Literature review: enteric nervous system development, genetic and epigenetic regulation in the etiology of Hirschsprung's disease. *Heliyon* 2021; 7: e07308.

[6] Ikawa H, Masuyama H, Hirabayashi T, Endo M and Yokoyama J. More than 10 years' follow-up of total colonic aganglionosis-severe iron deficiency anemia and growth retardation. *J Pediatr Surg* 1997; 32: 25-27.

[7] Workman MJ, Mahe MM, Trisno S, Poling HM, Watson CL, Sundaram N, Chang CF, Schiesser J, Aubert P, Stanley EG, Elefanty AG, Miyaoka Y, Mandegar MA, Conklin BR, Neunlist M, Bruggmann SA, Helmrath MA and Wells JM. Engineered human pluripotent-stem-cell-derived intestinal tissues with a functional enteric nervous system. *Nat Med* 2017; 23: 49-59.

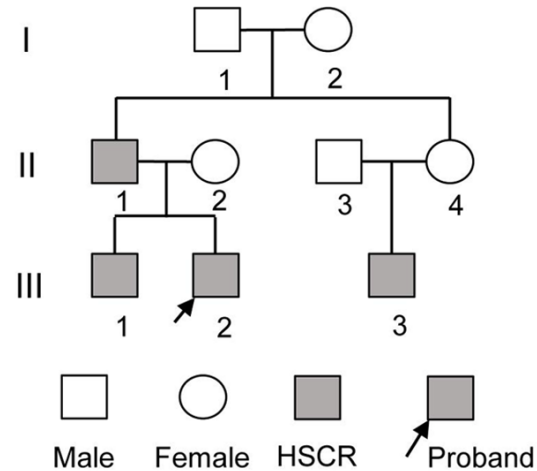
[8] Le TL, Galmiche L, Levy J, Suwannarat P, Hellebregers DM, Morarach K, Boismoreau F, Theunissen TE, Lefebvre M, Pelet A, Martinovic J, Gelot A, Guimiot F, Calleroz A, Gitiaux C, Hully M, Goulet O, Chardot C, Drunat S, Capri Y, Bole-Feysot C, Nitschke P, Whalen S, Mouthon L, Babcock HE, Hofstra R, de Coe IF, Tabet AC, Molina TJ, Keren B, Brooks A, Smeets HJ, Marklund U, Gordon CT, Lyonnet S, Amiel J and Bondurand N. Dysregulation of the NRG1/ERBB pathway causes a developmental disorder with gastrointestinal dysmotility in humans. *J Clin Invest* 2021; 131: e145837.

[9] Huang T, Hou Y, Wang X, Wang L, Yi C, Wang C, Sun X, Tam PKH, Ngai SM, Sham MH, Burns AJ

Pathogenicity of RET p.Phe147del in HSCR

- and Chan WY. Direct interaction of SOX10 with cadherin-19 mediates early sacral neural crest cell migration: implications for enteric nervous system development defects. *Gastroenterology* 2022; 162: 179-192, e111.
- [10] Wu W, Lu L, Xu W, Liu J, Sun J, Zheng L, Sheng Q and Lv Z. Whole exome sequencing identifies a novel pathogenic RET variant in hirschsprung disease. *Front Genet* 2018; 9: 752.
- [11] Tan K, Mo J, Li M, Dong Y, Han Y, Sun X, Ma Y, Zhu K, Wu W, Lu L, Liu J, Zhao K, Zhang L, Tang Y and Lv Z. SMAD9-MYCN positive feedback loop represents a unique dependency for MYCN-amplified neuroblastoma. *J Exp Clin Cancer Res* 2022; 41: 352.
- [12] Mo J, Tan K, Dong Y, Lu W, Liu F, Mei Y, Huang H, Zhao K, Lv Z, Ye Y and Tang Y. Therapeutic targeting the oncogenic driver EWSR1::FLI1 in Ewing sarcoma through inhibition of the FACT complex. *Oncogene* 2023; 42: 11-25.
- [13] Tan K, Wu W, Zhu K, Lu L and Lv Z. Identification and characterization of a glucometabolic prognostic gene signature in neuroblastoma based on N6-methyladenosine eraser ALKBH5. *J Cancer* 2022; 13: 2105-2125.
- [14] Mendelson A and Frenette PS. Hematopoietic stem cell niche maintenance during homeostasis and regeneration. *Nat Med* 2014; 20: 833-846.
- [15] Fantauzzo KA and Soriano P. Receptor tyrosine kinase signaling: regulating neural crest development one phosphate at a time. *Curr Top Dev Biol* 2015; 111: 135-182.
- [16] Vitiello PP, Cardone C, Martini G, Ciardiello D, Belli V, Matrone N, Barra G, Napolitano S, Della Corte C, Turano M, Furia M, Troiani T, Morgillo F, De Vita F, Ciardiello F and Martinelli E. Receptor tyrosine kinase-dependent PI3K activation is an escape mechanism to vertical suppression of the EGFR/RAS/MAPK pathway in KRAS-mutated human colorectal cancer cell lines. *J Exp Clin Cancer Res* 2019; 38: 41.
- [17] Machado RA, de Andrade RS, Pego SPB, Krepschi ACV, Coletta RD and Martelli-Junior H. New evidence of genetic heterogeneity causing hereditary gingival fibromatosis and ALK and CD36 as new candidate genes. *J Periodontol* 2023; 94: 108-118.
- [18] Sass JO, Behringer S, Fernando M, Cesaroni E, Cursio I, Volpini A and Till C. d-Glycerate kinase deficiency in a neuropsychiatric patient. *Brain Dev* 2020; 42: 226-230.
- [19] Coskun S, Karadag M, Gokcen C and Oztuzcu S. miR-132 and miR-942 expression levels in children with attention deficit and hyperactivity disorder: a controlled study. *Clin Psychopharmacol Neurosci* 2021; 19: 262-268.
- [20] Cagan Appak Y, Baran M, Ozturk Hismi B, Ozyilmaz B, Vardi K, Ozer Kaya O, Aksoy B and Kasap Demir B. Renal-hepatic-pancreatic dysplasia: an ultra-rare ciliopathy with a novel NPHP3 genotype. *J Pediatr Genet* 2020; 9: 101-103.
- [21] Zhao S, Huang C, Yang Y, Xu W, Yu Y, Wen C, Cao L, Gao F, Qin Y, Chen ZJ, Guo T and Zhao S. DNA repair protein FANCD2 has both ubiquitination-dependent and -independent functions during germ cell development. *J Biol Chem* 2023; 102905.
- [22] Nakatani T, Iwasaki M, Yamamichi A, Yoshioka Y, Uesaka T, Bitoh Y, Maeda K, Fukumoto T, Takemoto T and Enomoto H. Point mutagenesis in mouse reveals contrasting pathogenetic effects between MEN2B- and Hirschsprung disease-associated missense mutations of the RET gene. *Dev Growth Differ* 2020; 62: 214-222.
- [23] Gunadi, Dwihantoro A, Iskandar K, Makhmudi A and Rochadi. Accuracy of polymerase chain reaction-restriction fragment length polymorphism for RET rs2435357 genotyping as Hirschsprung risk. *J Surg Res* 2016; 203: 91-94.
- [24] Sunardi M, Ito K, Sato Y, Uesaka T, Iwasaki M and Enomoto H. A single RET mutation in Hirschsprung disease induces intestinal aganglionosis via a dominant-negative mechanism. *Cell Mol Gastroenterol Hepatol* 2022; [Epub ahead of print].
- [25] Mahato AK and Sidorova YA. RET receptor tyrosine kinase: role in neurodegeneration, obesity, and cancer. *Int J Mol Sci* 2020; 21: 7108.
- [26] van Weering DH and Bos JL. Glial cell line-derived neurotrophic factor induces Ret-mediated lamellipodia formation. *J Biol Chem* 1997; 272: 249-254.
- [27] Bishop JL, Thaper D and Zoubeidi A. The multifaceted roles of STAT3 signaling in the progression of prostate cancer. *Cancers (Basel)* 2014; 6: 829-859.
- [28] Plaza-Menacho I, van der Sluis T, Hollema H, Gimm O, Buys CH, Magee AI, Isacke CM, Hofstra RM and Eggen BJ. Ras/ERK1/2-mediated STAT3 Ser727 phosphorylation by familial medullary thyroid carcinoma-associated RET mutants induces full activation of STAT3 and is required for c-fos promoter activation, cell mitogenicity, and transformation. *J Biol Chem* 2007; 282: 6415-6424.
- [29] Kwon YT and Ciechanover A. The ubiquitin code in the ubiquitin-proteasome system and autophagy. *Trends Biochem Sci* 2017; 42: 873-886.

Pathogenicity of RET p.Phe147del in HSCR



Supplementary Figure 1. Pedigree of the three-generation Chinese family with four affected individuals. Squares indicate males and circles represent females. Black and white symbols represent affected and unaffected individuals, respectively. The proband is indicated by an arrow.

Supplementary Table 1. Information of 20 patients with Hirschsprung's disease

NO	Visiting age	Type	Operation age	Operation type	prognosis	Sanger results of RET p.Phe147del
1	1 month	Common	1 month	Soave	Good	No mutation
2	6 month	Common	6 month	Laparoscopic-assisted Soave	Good	No mutation
3	5 month	Common	5 month	Soave	Good	No mutation
4	1 month	Short segment	1 month	Soave	Good	No mutation
5	2 month	Common	2 month	Laparoscopic-assisted Soave	Good	No mutation
6	1 month	Common	1 month	Laparoscopic-assisted Soave	Good	No mutation
7	1 month	Short segment	1 month	Soave	Good	No mutation
8	2 month	Common	2 month	Laparoscopic-assisted Soave	Enterocolitis	No mutation
9	1 month	Long segment	1 month Fistulation 6 month Radical operation	Modified Duhamel	Occasional feces	No mutation
10	1 month	Long segment	1 month Fistulation 7 month Radical operation	Modified Duhamel	Good	No mutation
11	1 month	Whole segment	1 month Fistulation 5 month Radical operation	Modified Duhamel	Good	No mutation
12	2 month	Common	2 month	Laparoscopic-assisted Soave	Good	No mutation
13	half month	Short segment	half month	Soave	Good	No mutation
14	2 month	Common	2 month	Laparoscopic-assisted Soave	Enterocolitis	No mutation
15	1 month	Common	1 month	Soave	Good	No mutation
16	1 month	Short segment	1 month	Soave	Good	No mutation
17	1 month	Common	1 month	Laparoscopic-assisted Soave	Good	No mutation
18	1 month	Short segment	1 month	Soave	Good	mutation
19	1 month	Common	1 month	Laparoscopic-assisted Soave	Good	No mutation
20	1 month	Common	1 month	Laparoscopic-assisted Soave	Good	No mutation

Prognosis follow-up included defecation, enterocolitis, feces, etc.

Pathogenicity of RET p.Phe147del in HSCR

Supplementary Table 2. The basal information of autosomal chromosome mutation

Chr	Start	End	Ref	Alt
chr10	43597893	43597895	CTC	-
chr15	89850741	89850741	-	A
chr1	230916316	230916316	C	T
chr3	52325906	52325906	G	A
chr3	132418294	132418294	G	A
chr4	9784375	9784375	T	C
chr7	71868249	71868249	-	GG
chr20	57429470	57429470	G	C
chr21	37626146	37626146	C	G
chr22	18609484	18609484	G	T
chr22	20754984	20754984	C	T
chr3	66433559	66433559	C	T
chr3	69167989	69167989	G	T
chr3	150931834	150931834	C	T
chr4	8293256	8293256	G	A
chr4	20717736	20717736	G	T
chr7	38766568	38766568	C	T
chr7	100647186	100647186	A	C

Supplementary Table 3. The basal information of the main 18 mutated genes

Chr	Start	End	Ref	Alt	Func.refGene	Gene.refGene
chr10	43597893	43597895	CTC	-	exonic	RET
chr15	89850741	89850741	-	A	exonic	FANCI
chr1	230916316	230916316	C	T	exonic	CAPN9
chr3	52325906	52325906	G	A	exonic	GLYCTK
chr3	132418294	132418294	G	A	exonic; splicing	NPHP3; NPHP3
chr4	9784375	9784375	T	C	exonic	DRD5
chr7	71868249	71868249	-	GG	exonic	CALN1
chr20	57429470	57429470	G	C	exonic	GNAS
chr21	37626146	37626146	C	G	exonic	DOPEY2
chr22	18609484	18609484	G	T	exonic	TUBA8
chr22	20754984	20754984	C	T	exonic	ZNF74
chr3	66433559	66433559	C	T	exonic	LRIG1
chr3	69167989	69167989	G	T	exonic	LMOD3
chr3	150931834	150931834	C	T	exonic	P2RY14
chr4	8293256	8293256	G	A	exonic	HTRA3
chr4	20717736	20717736	G	T	exonic	PACRGL
chr7	38766568	38766568	C	T	exonic	VPS41
chr7	100647186	100647186	A	C	exonic	MUC12